

---

# CATS: Cascaded Adaptive Tree Speculation for Memory-Limited LLM Inference Acceleration

---

**Yuning Han**  
University of Florida  
Gainesville, FL 32611  
yuninghan@ufl.edu

**Yangchenchen Jin**  
University of Florida  
Gainesville, FL 32611  
yangchenchen.jin@ufl.edu

**Dylan Zhao**  
University of Florida  
Gainesville, FL 32611  
dylan.zhao@ufl.edu

**Jingwei Sun**  
University of Florida  
Gainesville, FL 32611  
sun.jingwei@ufl.edu

## Abstract

Auto-regressive decoding in Large Language Models (LLMs) is inherently memory-bound: every generation step requires loading the model weights and intermediate results from memory (e.g., High-Bandwidth Memory (HBM) for GPU servers), making throughput bottlenecked by memory bandwidth rather than compute. Speculative decoding addresses this by enabling parallel verification of multiple draft tokens, effectively amortizing the cost of each target-model call. However, existing speculative decoding methods are designed under the assumption that HBM is sufficiently large to hold both the target model and an auxiliary draft model simultaneously—an assumption that breaks down on memory-constrained devices such as edge platforms with limited DRAM. We analyze the inference bottleneck in this memory-limited regime and propose CATS, a self-speculative decoding framework that conducts cascaded verification and correction based on the memory budget and parameter offloading patterns on memory-limited devices. This design maximizes token acceptance rate and end-to-end speedup while keeping the peak memory footprint on the device equal to that of the target model alone. We evaluate CATS on different models across five benchmarks on real edge devices. CATS can achieve a wall-clock speedup of up to  $5.08\times$  with no degradation in generation quality, outperforming the SOTA method by up to  $1.45\times$  under edge memory constraints. Code is available at <https://github.com/ElizaFuLan/CATS.git>.

## 1 Introduction

Deploying Large Language Models (LLMs) for efficient inference remains one of the central challenges in modern machine learning systems. LLM inference must generate tokens one at a time in an autoregressive loop—each step conditioned on all prior outputs and requiring a full model forward pass. This sequential structure is inherently memory-bound: every generation step loads the model weights and intermediate results from memory (e.g., High-Bandwidth Memory (HBM) for GPU servers) to on-chip compute units, and throughput is governed by memory bandwidth rather than arithmetic capacity [1, 2]. Speculative decoding was proposed to break this bottleneck through *parallel decoding* [3, 4, 5]: a lightweight draft model speculatively generates a sequence of candidate tokens, which the larger target model then verifies in a single batched forward pass. Because the target model processes multiple tokens simultaneously, the per-token memory bandwidth cost is amortized over several accepted tokens, substantially improving throughput while preserving the exact output distribution.

However, this throughput gain comes at a structural cost: classical speculative decoding introduces a *second* set of weights—the auxiliary draft model—that must coexist with the target model in device memory, inflating both the static memory footprint and the per-step bandwidth traffic. Self-speculative decoding methods [6, 7, 8, 9] emerged as a practical response to this added memory cost: by generating drafts from a shallow sub-network of the target model itself, they eliminate the need for a separate draft model. However, they still need to introduce additional adapter parameters for drafting, and the performance of these methods often suffers from the sub-network’s limited drafting capacity.

A more fundamental limitation runs through *all* existing speculative decoding approaches: they assume model weights remain resident in device memory (e.g., HBM for servers and DRAM for edge devices) for the duration of inference. On large-scale servers, this holds, but on memory-limited platforms such as edge devices, DRAM capacity falls well short of a single 7B-parameter model and must be shared with the operating system—so weights must be streamed from flash memories on every forward pass [2], making flash↔DRAM the rate-limiting transfer rather than DRAM↔on-chip memory. Every design choice in existing methods—draft depth, verification strategy, acceptance policy—targets the memory-resident regime and is misaligned with this memory-constrained setting. Auxiliary-model approaches are doubly penalized: maintaining a separate draft model adds memory capacity demands and extra transfer traffic at every speculative step, compounding the bottleneck they were meant to relieve.

We investigate this memory-limited inference bottleneck and propose CATS (Cascaded Adaptive Tree Speculation), a self-speculative decoding framework that performs cascaded verification to minimize inference time within the memory budget. CATS organizes inference into three stages whose layer boundaries are determined by the available DRAM budget: (1) a **draft** stage using a shallow sub-network to draft candidate tokens by repeating draft iterations; (2) a **shallow verification** stage using intermediate layers under the DRAM budget, streamed from flash once per cycle, to check draft tokens and produce correction candidates in parallel; and (3) a **target verify** stage where the remaining layers are offloaded from the flash chunk by chunk to process a tree-structured input over the draft trace and all correction branches to select the longest accepted prefix. We also propose a **Reduced KL Loss** that focuses distillation supervision on high-probability tokens to maximize the sub-network’s drafting and verification capabilities.

Our main contributions are as follows:

- We identify flash↔DRAM data movement as the dominant bottleneck for speculative decoding on edge devices—a constraint entirely overlooked by existing methods—and propose CATS, a cascaded self-speculative decoding framework for this memory-constrained regime.
- CATS is **model-agnostic**: the cascaded framework applies to any transformer-based LLM without architectural modifications.
- We implement our framework on edge devices. Extensive experiments on Vicuna-7B/13B and LLaMA2-7B/13B across five benchmarks demonstrate that CATS achieves up to **5.08**× speedup, outperforming all compared self-speculative decoding baselines including KANGAROO [9], MEDUSA [10], and EAGLE [11] under the memory-limited setting.

## 2 Related Work

**Speculative decoding with auxiliary draft models.** The canonical speculative decoding framework [3, 4, 12] relies on a separately trained smaller model to propose candidates that the target model verifies in parallel. Subsequent work has extended this to tree-structured verification [13, 14, 15, 16], knowledge-distilled draft models [17, 18, 19], retrieval-based drafting [20, 21, 22], and lookahead generation [23]; see [24] for a comprehensive survey. Methods that rely on independently trained

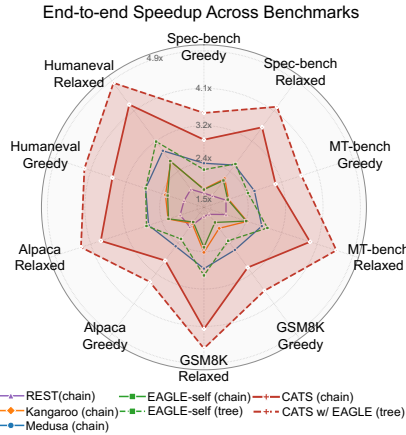


Figure 1: End-to-end speedup across five benchmarks on Vicuna-7B.

smaller models [25, 26, 27, 28, 29, 30, 31, 32, 33, 34, 35] incur significant memory overhead, a challenge in edge scenarios where even the target model barely fits in device memory.

**Self-speculative decoding.** To eliminate the dependency on a separate draft model, a line of *self-speculative* methods derives the draft model directly from the target model’s own layers. Early-exit approaches such as DRAFT & VERIFY [6] and LAYERSKIP [7] route tokens through only the first few transformer layers for drafting and use the full model for verification. SWIFT [8] selects skip layers dynamically per input without fine-tuning, while KNAPSPEC [36] formulates layer selection as a knapsack optimization problem. KANGAROO [9] introduces a lightweight adapter on top of the shallow sub-network trained to mimic the target model’s output distribution, achieving strong acceptance rates with minimal overhead. Multi-head approaches such as MEDUSA [10] and HYDRA [37] attach parallel prediction heads to the target model’s final layer, enabling several future tokens to be proposed in a single forward pass. The EAGLE series [11, 38, 39] drafts at the feature level and constructs dynamic token trees, achieving state-of-the-art speedups on server-class hardware. Consistency-based training [40, 41] and multi-token prediction objectives [42, 43, 44] provide complementary approaches for parallel generation. A common limitation across all these methods is that they still require additional adapter parameters for drafting, which can diminish the performance gains in memory-limited settings achieved by existing speculative decoding methods. And the performance of these methods often suffers from the sub-network’s limited drafting capacity.

**LLM inference on memory-constrained hardware.** LLM in a Flash [2] characterizes the flash-memory $\leftrightarrow$ DRAM bandwidth bottleneck on edge devices where model weights cannot reside in DRAM and proposes windowed loading and row-column bundling to reduce transfer volume per forward pass. PowerInfer [45] exploits activation sparsity to selectively load only hot neurons. These works [46, 47] recognize the memory bottleneck as the critical constraint on edge inference — a constraint that our method seeks to address for existing speculative decoding methods in the same setting.

### 3 Preliminary and Motivation

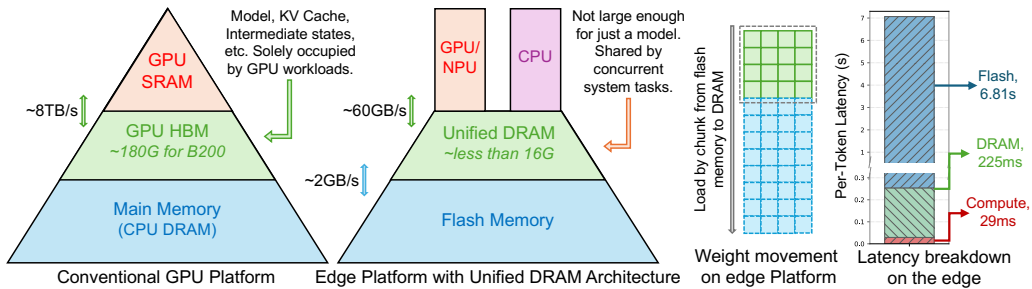


Figure 2: Memory hierarchy on server vs. edge, with measured per-token latency breakdown for autoregressive Vicuna-7B inference. *Server (B200)*: model weights reside in HBM; the binding bottleneck is HBM $\leftrightarrow$ SRAM bandwidth, and per-token latency is compute-dominated. *Edge (Jetson AGX Orin)*: DRAM cannot hold the full model, so weights must be staged from flash on every forward pass; flash $\leftrightarrow$ DRAM transfer dominates per-token latency.

The structural mismatch identified in Section 1—that all speculative decoding methods assume memory-resident weights, a condition that fails on edge—stems from a fundamental difference in memory hierarchy between the two deployment regimes, which Figure 2 makes explicit. On a conventional GPU platform (e.g., NVIDIA B200), HBM provides  $\sim 180$  GB at  $\sim 8$  TB/s, comfortably holding the target model, an auxiliary draft model, and all intermediate states simultaneously; the binding cost during decoding is the fast HBM $\leftrightarrow$ SRAM path. On an edge platform with a unified DRAM architecture, the GPU/NPU and CPU share a single DRAM pool of  $\lesssim 16$  GB—difficult to host even a single 7B-parameter model ( $\sim 14$  GB), let alone an extra draft model. The data between DRAM and the flash memory moves at only  $\sim 2$  GB/s. During the inference, model weights must be loaded chunk by chunk from flash into DRAM on every forward pass [2], and the binding bottleneck

shifts to this flash $\leftrightarrow$ DRAM movement as reflected in the latency breakdown in Figure 2. This bottleneck shift makes the existing speculative decoding methods inferior in memory-limited settings. We perform profiling on AGX Orin devices with limited memory budget and visualize this effect in Figure 3: the end-to-end speedup of Kangaroo and EAGLE drops by 19.8% and 24.5%, respectively, when moving from server to edge, compared to vanilla inference on corresponding platforms. This effect is more severe for methods like EAGLE that introduce an additional draft model, since these components must also be staged through the constrained edge memory hierarchy.

## 4 Methodology

In this section, we formalize the memory-adaptive three-stage inference framework that is central to CATS and describe its three-stage inference pipeline. We then detail the verification tree construction and the Reduced KL Loss used to train the draft and shallow-verifier adapters. The detailed algorithm can be found in Appendix A.

### 4.1 Notation

We use *target model* (TM) for the target LLM, *draft model* (DM) for layers 1 to  $L_{DM}$  plus a lightweight adapter, which is well-trained to transform the shallow-layer outputs of the TM into calibrated representations suitable for next-token prediction, and *shallow verifier* (SV) for layers  $L_{DM}+1$  to  $L_{SV}$  plus its adapter. A forward through layers 1 to  $L_{DM}$  is a *drafting pass*, through  $L_{DM}+1$  to  $L_{SV}$  an *SV pass*, and through  $L_{SV}+1$  to  $L_{final}$  the *final pass*;  $\bar{\gamma}$  denotes the number of drafting passes per decoding cycle. Here,  $L_{DM}$  denotes the draft boundary, i.e., the last layer included in the draft model;  $L_{SV}$  denotes the shallow-verification boundary, i.e., the last layer used by the shallow verifier; and  $L_{final}$  denotes the final layer of the target model.

### 4.2 Cascaded verification design

The left part of Figure 4 illustrates the full CATS pipeline. Each decoding cycle alternates between flash-to-DRAM weight movement and computation across three stages. In this paper, we focus on weight movement because edge inference is typically latency-oriented and operates at small batch sizes, where the KV cache is not the dominant memory consumer as in large-batch serving. When KV-cache pressure becomes relevant, it can be treated as part of the streamed state alongside model weights, so the same memory-adaptive scheduling principle still applies.

**Drafting loop.** CATS uses a compact DM that is small enough to fit within the DRAM budget of the edge device. The draft boundary  $L_{DM}$  is chosen not simply to maximize the number of layers that can be loaded into DRAM, but to balance three constraints: DRAM capacity, limited edge compute throughput, and memory bandwidth. A deeper draft model may improve the drafting quality, but it also increases the cost of each auto-regressive drafting step. We therefore keep the draft model intentionally shallow and perform  $\bar{\gamma}$  sequential drafting passes to generate  $\bar{\gamma}$  candidate tokens with reasonable latency. To preserve draft quality under this small-model constraint, the draft adapter is trained with the reduced KL loss introduced later.

**Shallow verification pass.** The shallow verifier boundary is adaptively chosen according to memory budgets, which means that the medium sub-network (layers  $L_{DM} + 1$  through  $L_{SV}$ ) will be moved to DRAM along with the draft model during the first flash to DRAM movement for each cycle. The  $\bar{\gamma}$  candidates are then forwarded in parallel through these intermediate layers, and the SV adapter decodes a verification token at each position. Each SV token is compared strictly against the corresponding draft token: matching positions are passed through to the target stage; mismatching positions yield a correction candidate. When mismatches happen, the draft tokens and corrections are assembled into a verification tree as shown in Figure 4. The correction tokens are then re-forwarded from layer 1 through  $L_{SV}$  under tree-masked attention to get the hidden states of the correction

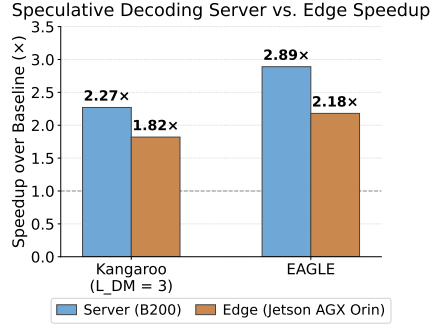


Figure 3: End-to-end speedup of speculative decoding methods on B200 vs. Jetson AGX Orin.

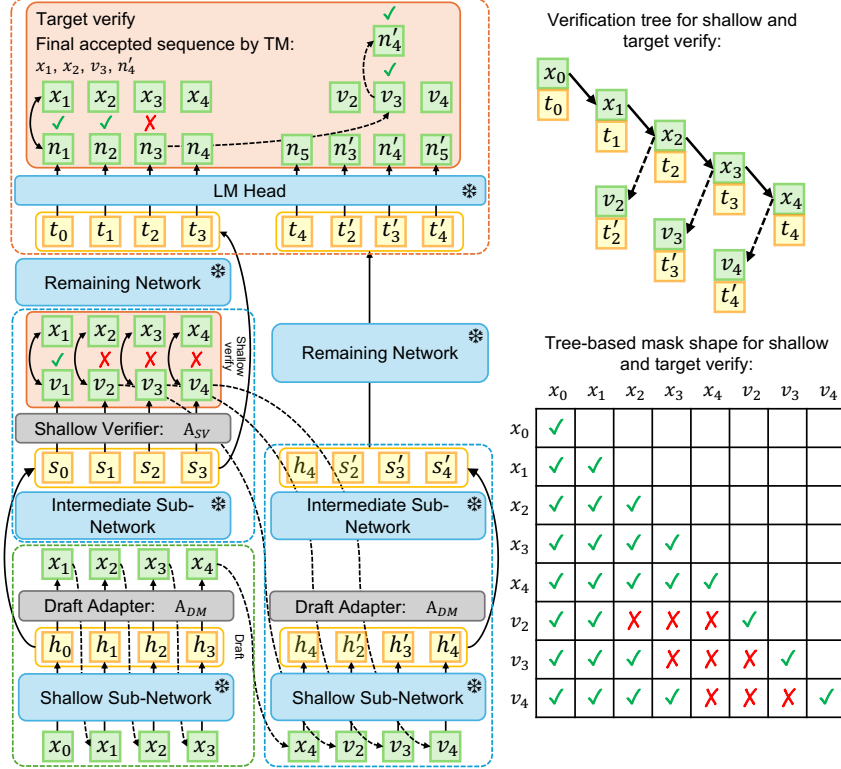


Figure 4: Pipeline of CATS. **Left**: three-stage decoding cycle showing the interleaved flash↔DRAM transfers and GPU computation. The bottommost blue block (draft sub-network) and the intermediate SV layers (middle blue block) are streamed from flash once per full inference cycle during the drafting and shallow verification process (regarded as a SD process); the target layers (top blue block, rest of the models) are streamed accordingly during the final pass. Green blocks: token embeddings; yellow blocks: hidden states; yellow-bordered box: parallel forward computation; orange blocks: verification decision. Draft and SV adapter structure follows [9]. **Right upper**: verification tree structure. **Right lower**: tree-based attention mask encoding the main draft sequence and SV correction branches for the batched final pass.

token—reusing the already-loaded draft and SV layers—at zero additional flash transfer cost. The insight of this DM-to-SV stage is to serve as an internal speculative decoding process that fully exploits the limited DRAM capacity.

**Target verification pass.** The remaining layers  $L_{SV}+1$  through  $L_{total}$  are then streamed from flash into DRAM chunk by chunk in the rest of the sequential transfer. The assembled verification tree is processed in a single batched forward pass under the corresponding tree attention mask. The target model can verify the main draft branch following greedy decoding or via typical acceptance [10]; at each rejected position, the SV’s correction candidate is evaluated under the same criterion. The longest accepted prefix is committed to the output, and the KV cache is updated accordingly.

### 4.3 Adapter design and training

Draft and verification adapters follow the architecture of [9]: two normalization layers, one multi-head attention layer, and a shared LM head. Because CATS uses compact draft and shallow-verifier sub-networks to meet edge device memory and latency constraints, their drafting and verification ability must be strengthened under limited sub-model capacity. Rather than distilling the full vocabulary from the full model [17, 9], which wastes supervision on low-probability tokens that rarely affect acceptance, we train the adapters with a **Reduced KL Loss** that focuses on the tokens most relevant to accepted tokens.

A general distillation loss that aligns the adapter distribution with the target model over the entire vocabulary is formed as:

$$\mathcal{L}_{\text{full}} = -\frac{1}{|M|} \sum_{t \in M} \sum_{v=1}^V p_{\text{target}}(v | t) \cdot \log q_{\text{draft}}(v | t), \quad (1)$$

where  $M$  is the set of unmasked token positions,  $p_{\text{target}}$  is the target model’s distribution, and  $q_{\text{draft}}$  is the adapter’s distribution. Spreading supervision across the full vocabulary  $V$  dilutes the gradient signal onto near-zero-mass tokens that are irrelevant to accepted tokens. We instead restrict it to the top- $K$  tokens:

$$\mathcal{L}_{\text{top-}K} = -\frac{1}{|M|} \sum_{t \in M} \sum_{v \in \mathcal{T}_K(t)} \tilde{p}_{\text{target}}(v | t) \cdot \log q_{\text{draft}}(v | t) \quad (2)$$

where  $\mathcal{T}_K(t)$  denotes the set of top- $K$  tokens under the target distribution at position  $t$ , and  $\tilde{p}_{\text{target}}(v | t)$  is the target distribution renormalized over this set. This concentrates distillation on the tokens that actually determine acceptance while excluding the low-probability tail. The detailed computation process can be found in Appendix B.

## 5 Experiments

**Models, tasks, baselines, and metrics.** We conducted experiments on Vicuna models (7B and 13B) [48] and LLaMA2 models (7B and 13B) [49], which are mainstream LLMs widely tested on different self-speculative decoding algorithms. We evaluated CATS across multiple tasks, including multi-turn dialogue, code generation, mathematical reasoning, and instruction following, using Spec-bench [24], MT-bench [50], GSM8K [51], Alpaca [52], and HumanEval [53].

Unless otherwise stated, we set the drafting steps  $\bar{\gamma} = 5$ , choose a compact draft boundary  $L_{\text{DM}}=3$ , and set the shallow-verifier boundary to  $L_{\text{SV}}=15$ . Following the design principle in Section 4,  $L_{\text{DM}}$  is kept shallow to balance DRAM capacity, compute throughput, and repeated drafting cost, while  $L_{\text{SV}}=15$  corresponds to representative edge-memory budgets of 8 GB for 7B models and 12 GB for 13B models. We compare against representative speculative decoding algorithms, including REST [20], Lookahead decoding [23], Kangaroo [9], Medusa [10], and EAGLE [11]. Since our cascaded verification framework is orthogonal to EAGLE’s high-probability candidate branching, CATS w/ EAGLE adds these branches to our verification tree to enlarge the parallel candidate set without additional target-model forward passes.

We report the mean accepted length and end-to-end speedup. Mean accepted length measures the average number of tokens accepted per target-model verification, which is irrelevant to the deployed platform, while end-to-end speedup captures the wall-clock acceleration on the target platform. We use a server with 8 B200 GPUs to obtain mean accepted length results, and an NVIDIA Jetson AGX Orin as the edge device for end-to-end speedup evaluation.

**Training.** For fine-tuning our own adapters, we used the ShareGPT dataset [48] with 68,000 samples following Medusa, with learning rate set at 1e-6 for Vicuna 7B and 13B models, and 1e-5 for LLaMA2 7B and 13B models separately. All the trainings are finished with 2 B200 GPUs within 13 hours.

### 5.1 Main results

**Mean accepted length and end-to-end speedup.** Tables 1 and 2 report the main results. Since EAGLE was originally designed around feature-level speculative decoding, we re-implement it in our self-speculative setting and evaluate both decoding modes: chain decoding and tree decoding. In the edge setting, where each decoding loop is constrained by limited compute and weight-transfer bandwidth, increasing the mean accepted length directly reduces the number of costly inference loops and is reflected in the measured end-to-end speedup.

Table 1 reports results on Vicuna-7B under both greedy and relaxed decoding. Under greedy decoding, CATS accepts 3.06 tokens per target call on average, compared with 2.49 for Kangaroo, 2.48 for Medusa, and 2.47 for our self-speculative EAGLE chain baseline—a 23–24% relative gain. This translates into a 3.18× end-to-end speedup, 66% higher than Kangaroo’s 1.92×. Compared with the full-baseline Lookahead and REST, CATS improves mean accepted length by 29% and 79%, respectively. Under relaxed decoding ( $\tau=0.7$ ), these gains are maintained or amplified: CATS

Table 1: Mean accepted length ( $\tau$ ) and end-to-end speedup ( $S \uparrow$ ) on Vicuna-7B across five benchmarks under greedy and relaxed (temperature=0.7) decoding. Kangaroo and CATS use drafting steps = 5; Medusa uses 2 heads; EAGLE is re-implemented in a self-speculative structure with drafting steps = 5. In tree base decoding, we set top- $K$  = 10. Lookahead is greedy-only.

Model	Algorithm	Spec-bench		MT-bench		GSM8K		Alpaca		HumanEval		Mean	
		$\tau$	$S \uparrow$	$\tau$	$S \uparrow$	$\tau$	$S \uparrow$	$\tau$	$S \uparrow$	$\tau$	$S \uparrow$	$\tau$	$S \uparrow$
Greedy													
Vicuna-7b chain base	REST[20]	1.6243	1.66×	1.8239	1.86×	1.5045	1.54×	1.8406	1.88×	1.7670	1.81×	1.7121	1.75×
	Lookahead[23]	2.2785	2.29×	2.2928	2.30×	2.7010	2.72×	2.0623	2.08×	2.5128	2.53×	2.3695	2.38×
	Kangaroo[9]	2.2736	1.75×	2.4863	1.92×	2.4856	1.92×	2.3131	1.79×	2.8979	2.24×	2.4914	1.92×
	Medusa[10]	2.3116	2.32×	2.5115	2.52×	2.4966	2.51×	2.3917	2.41×	2.6832	2.70×	2.4789	2.49×
	EAGLE-self[11]	2.2995	1.74×	2.5151	1.90×	2.3213	1.76×	2.3104	1.75×	2.9005	2.19×	2.4694	1.87×
CATS	<b>2.8816</b>	<b>2.99×</b>	<b>3.0520</b>	<b>3.16×</b>	<b>3.0198</b>	<b>3.14×</b>	<b>2.8280</b>	<b>2.94×</b>	<b>3.5174</b>	<b>3.65×</b>	<b>3.0598</b>	<b>3.18×</b>	
Vicuna-7b tree base	EAGLE-self, tree	2.8943	2.18×	3.1535	2.37×	3.0059	2.26×	2.9306	2.21×	3.5949	2.70×	3.1158	2.34×
	CATS w/ EAGLE	<b>3.5097</b>	<b>3.51×</b>	<b>3.6938</b>	<b>3.69×</b>	<b>3.6869</b>	<b>3.70×</b>	<b>3.4339</b>	<b>3.45×</b>	<b>4.2009</b>	<b>4.21×</b>	<b>3.7050</b>	<b>3.71×</b>
Relaxed (temperature = 0.7)													
Vicuna-7b chain base	REST	1.6236	1.66×	1.8216	1.86×	1.5192	1.55×	1.8594	1.90×	1.7984	1.84×	1.7244	1.76×
	Kangaroo	2.7777	2.13×	3.0712	2.35×	3.0513	2.34×	2.8348	2.18×	3.3703	2.59×	3.0211	2.32×
	Medusa	2.4884	2.50×	2.6802	2.69×	2.6837	2.70×	2.6179	2.63×	2.8760	2.89×	2.6692	2.68×
	EAGLE-self	2.7487	2.08×	3.0753	2.33×	2.9515	2.23×	2.8644	2.17×	3.4546	2.61×	3.0189	2.28×
	CATS	<b>3.4791</b>	<b>3.60×</b>	<b>3.7597</b>	<b>3.89×</b>	<b>3.9652</b>	<b>4.12×</b>	<b>3.6742</b>	<b>3.82×</b>	<b>4.0802</b>	<b>4.24×</b>	<b>3.7917</b>	<b>3.94×</b>
Vicuna-7b tree base	EAGLE-self	3.3494	2.53×	3.7271	2.82×	3.7629	2.85×	3.5334	2.68×	4.1547	3.14×	3.7055	2.80×
	CATS w/ EAGLE	<b>4.1802</b>	<b>4.18×</b>	<b>4.5229</b>	<b>4.52×</b>	<b>4.5345</b>	<b>4.55×</b>	<b>4.2745</b>	<b>4.29×</b>	<b>4.8408</b>	<b>4.85×</b>	<b>4.4706</b>	<b>4.48×</b>

Table 2: Mean accepted length ( $\tau$ ) and end-to-end speedup ( $S \uparrow$ ) on Vicuna-13B and LLaMA2-7B/13B under greedy and relaxed (temperature = 0.7) decoding. Methods and settings follow Table 1.

Model	Algorithm	Spec-bench		MT-bench		GSM8K		Alpaca		HumanEval		Mean	
		$\tau$	$S \uparrow$	$\tau$	$S \uparrow$	$\tau$	$S \uparrow$	$\tau$	$S \uparrow$	$\tau$	$S \uparrow$	$\tau$	$S \uparrow$
Greedy													
Vicuna-13b chain base	Kangaroo	2.1937	2.19×	2.4184	2.41×	2.3848	2.38×	2.2226	2.22×	2.9183	2.91×	2.4276	2.42×
	Medusa	2.3920	2.03×	2.5833	2.19×	2.5824	2.20×	2.3959	2.04×	2.8035	2.39×	2.5514	2.17×
	EAGLE-self	2.1952	2.18×	2.3831	2.37×	2.2031	2.19×	2.2183	2.21×	2.9163	2.90×	2.3832	2.37×
	CATS	<b>2.6588</b>	<b>2.64×</b>	<b>2.7946</b>	<b>2.77×</b>	<b>2.7636</b>	<b>2.74×</b>	<b>2.5493</b>	<b>2.53×</b>	<b>3.2218</b>	<b>3.20×</b>	<b>2.7976</b>	<b>2.78×</b>
Vicuna-13b tree base	EAGLE-self, tree	2.8035	2.77×	3.0423	3.01×	2.8760	2.85×	2.8337	2.81×	3.6168	3.58×	3.0345	3.00×
	CATS w/ EAGLE	<b>3.4708</b>	<b>3.42×</b>	<b>3.6897</b>	<b>3.64×</b>	<b>3.5481</b>	<b>3.50×</b>	<b>3.3568</b>	<b>3.32×</b>	<b>4.2428</b>	<b>4.19×</b>	<b>3.6616</b>	<b>3.61×</b>
Llama2-7b chain base	Kangaroo	3.8176	3.29×	4.1930	3.61×	4.4296	3.82×	4.0431	3.49×	4.2946	3.70×	4.1534	3.58×
	Medusa	1.6660	1.67×	1.7817	1.78×	1.7358	1.74×	1.7758	1.78×	1.9657	1.97×	1.7850	1.78×
	EAGLE-self	3.8068	3.28×	4.1813	3.60×	4.7597	4.10×	4.0429	3.49×	4.0588	3.50×	4.1699	3.60×
	CATS	<b>4.3335</b>	<b>4.33×</b>	<b>4.6181</b>	<b>4.62×</b>	<b>5.1055</b>	<b>5.10×</b>	<b>4.4642</b>	<b>4.46×</b>	<b>4.7240</b>	<b>4.72×</b>	<b>4.6491</b>	<b>4.65×</b>
Llama2-7b tree base	EAGLE-self, tree	4.3529	3.75×	4.7199	4.07×	5.0954	4.39×	4.5393	3.91×	4.5866	3.95×	4.6588	4.02×
	CATS w/ EAGLE	<b>4.8318</b>	<b>4.83×</b>	<b>5.0634</b>	<b>5.06×</b>	<b>5.4185</b>	<b>5.42×</b>	<b>4.9101</b>	<b>4.91×</b>	<b>5.1741</b>	<b>5.17×</b>	<b>5.0796</b>	<b>5.08×</b>
Llama2-13b chain base	Kangaroo	3.5409	3.53×	3.9369	3.92×	4.2421	4.23×	3.9754	3.97×	4.1133	4.10×	4.1534	3.95×
	Medusa	1.8250	1.55×	1.9737	1.68×	1.9721	1.68×	1.9425	1.65×	1.9425	1.65×	1.9312	1.64×
	EAGLE-self	3.5478	3.53×	3.9754	3.96×	3.8572	3.84×	3.9805	3.97×	4.1082	4.09×	3.8938	3.88×
	CATS	<b>4.0570</b>	<b>4.02×</b>	<b>4.2752</b>	<b>4.24×</b>	<b>4.3415</b>	<b>4.31×</b>	<b>4.3696</b>	<b>4.34×</b>	<b>4.6959</b>	<b>4.66×</b>	<b>4.3478</b>	<b>4.32×</b>
Llama2-13b tree base	EAGLE-self, tree	4.0829	4.04×	4.4699	4.42×	4.2793	4.24×	4.4566	4.42×	4.6993	4.65×	4.3976	4.35×
	CATS w/ EAGLE	<b>4.5707</b>	<b>4.51×</b>	<b>4.8191</b>	<b>4.75×</b>	<b>4.8534</b>	<b>4.79×</b>	<b>4.7998</b>	<b>4.75×</b>	<b>5.0178</b>	<b>4.95×</b>	<b>4.8122</b>	<b>4.75×</b>
Relaxed (temperature = 0.7)													
Vicuna-13b chain base	Kangaroo	2.4889	2.48×	2.7894	2.78×	2.7695	2.76×	2.5927	2.59×	3.2753	3.27×	2.7832	2.78×
	Medusa	2.5852	2.20×	2.7905	2.37×	2.7920	2.38×	2.7148	2.31×	2.9535	2.51×	2.7672	2.35×
	EAGLE-self	2.5144	2.50×	2.8444	2.83×	2.5893	2.58×	2.6609	2.65×	3.2212	3.20×	2.7660	2.75×
	CATS	<b>2.9743</b>	<b>2.95×</b>	<b>3.2421</b>	<b>3.22×</b>	<b>3.0736</b>	<b>3.05×</b>	<b>2.9963</b>	<b>2.98×</b>	<b>3.4792</b>	<b>3.45×</b>	<b>3.1531</b>	<b>3.13×</b>
Vicuna-13b tree base	EAGLE-self, tree	3.1934	3.16×	3.5232	3.49×	3.3631	3.33×	3.3051	3.28×	3.9784	3.94×	3.4726	3.44×
	CATS w/ EAGLE	<b>3.9851</b>	<b>3.93×</b>	<b>4.2360</b>	<b>4.18×</b>	<b>4.1399</b>	<b>4.09×</b>	<b>4.0683</b>	<b>4.02×</b>	<b>4.7269</b>	<b>4.67×</b>	<b>4.2312</b>	<b>4.18×</b>
Llama2-7b chain base	Kangaroo	4.4849	3.87×	4.9609	4.28×	4.8506	4.18×	4.9796	4.29×	4.0587	3.50×	4.6669	4.02×
	Medusa	1.7482	1.75×	1.8667	1.87×	2.1875	2.19×	1.8955	1.90×	2.2848	2.28×	1.9965	2.00×
	EAGLE-self	4.4910	3.87×	4.9756	4.29×	4.9139	4.24×	4.9867	4.30×	4.2687	3.68×	4.7272	4.08×
	CATS	<b>4.8831</b>	<b>4.88×</b>	<b>5.2004</b>	<b>5.20×</b>	<b>5.1870</b>	<b>5.19×</b>	<b>5.1976</b>	<b>5.20×</b>	<b>4.4388</b>	<b>4.44×</b>	<b>4.9814</b>	<b>4.98×</b>
Llama2-7b tree base	EAGLE-self, tree	4.9713	4.29×	5.2409	4.52×	5.2814	4.55×	5.3228	4.59×	4.7703	4.11×	5.1173	4.41×
	CATS w/ EAGLE	<b>5.3143</b>	<b>5.31×</b>	<b>5.5818</b>	<b>5.58×</b>	<b>5.5096</b>	<b>5.51×</b>	<b>5.5601</b>	<b>5.56×</b>	<b>4.9882</b>	<b>4.99×</b>	<b>5.3908</b>	<b>5.39×</b>
Llama2-13b chain base	Kangaroo	4.1486	4.14×	4.6991	4.68×	4.6031	4.59×	4.7376	4.73×	4.6950	4.68×	4.5767	4.56×
	Medusa	1.9322	1.64×	2.0646	1.75×	2.2499	1.92×	2.0718	1.76×	2.2848	1.95×	2.1207	1.80×
	EAGLE-self	4.1452	4.12×	4.7032	4.68×	4.5883	4.57×	4.7401	4.72×	4.7135	4.69×	4.5781	4.56×
	CATS	<b>4.6461</b>	<b>4.61×</b>	<b>4.9133</b>	<b>4.87×</b>	<b>5.3102</b>	<b>5.27×</b>	<b>4.9464</b>	<b>4.92×</b>	<b>5.0678</b>	<b>5.03×</b>	<b>4.9768</b>	<b>4.94×</b>
Llama2-13b tree base	EAGLE-self, tree	4.7176	4.67×	5.1051	5.05×	5.1449	5.10×	5.0338	4.99×	5.1758	5.12×	5.0354	4.98×
	CATS w/ EAGLE	<b>5.0813</b>	<b>5.01×</b>	<b>5.3499</b>	<b>5.28×</b>	<b>5.5524</b>	<b>5.48×</b>	<b>5.3241</b>	<b>5.27×</b>	<b>5.3969</b>	<b>5.33×</b>	<b>5.3409</b>	<b>5.27×</b>

continues to lead all baselines including REST, whose relaxed-acceptance advantage over greedy is outpaced by the longer draft sequences that CATS produces. Table 2 extends the evaluation to Vicuna-13B and LLaMA2-7B/13B under both decoding modes. On LLaMA2-7B, CATS reaches 4.65 accepted tokens and 4.65 $\times$  speedup under greedy decoding, versus 4.17 tokens (3.60 $\times$ ) for the EAGLE chain baseline and 4.15 tokens (3.58 $\times$ ) for Kangaroo. On the larger LLaMA2-13B, CATS achieves 4.35 accepted tokens and 4.32 $\times$  speedup, compared with 3.89 (3.88 $\times$ ) for EAGLE-self and 3.96 (3.95 $\times$ ) for Kangaroo. Pairing CATS with EAGLE tree decoding further pushes accepted length to 5.08 and 4.81 tokens on LLaMA2-7B and 13B, respectively, with corresponding speedups of 5.08 $\times$  and 4.75 $\times$ . These consistent gains across model families and sizes confirm that the cascaded verification advantage is not model-specific.

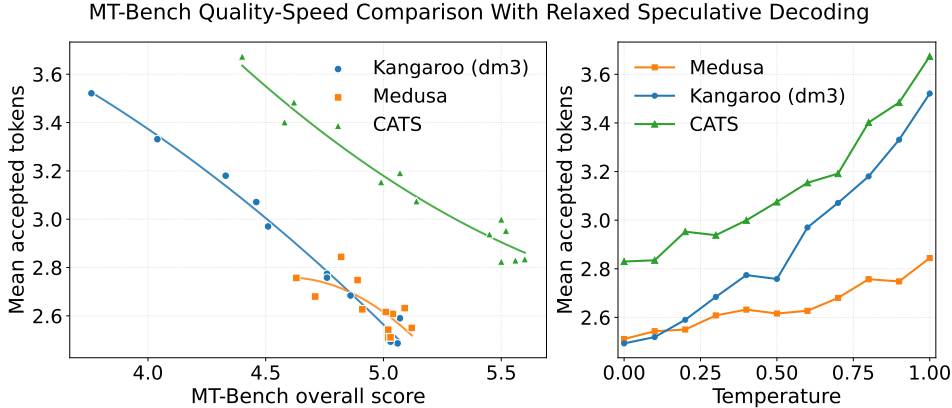


Figure 5: MT-Bench quality–speed comparison under relaxed acceptance. Quality is measured by the GPT-4o following the protocol of [50]; we report the mean score across all MT-Bench categories.

**Quality–speed Pareto frontier.** A common concern with relaxed speculative decoding is that increasing the number of accepted draft tokens may improve speed at the expense of generation quality. Figure 5 shows that this trade-off is not inherent to CATS. Under matched schedules ( $\tau=0.3$ ,  $\alpha=0.09$ , 5 draft steps), CATS lies on the upper-right Pareto frontier on MT-Bench, improving accepted length while maintaining competitive evaluation scores. Sweeping temperature from 0 to 1 preserves the separation, suggesting that cascaded verification increases usable parallelism without relaxing the target distribution.

## 5.2 Ablation Study

In ablation studies, we examine how CATS behaves under the two constraints that dominate limited memory deployment: memory budget and auto-regressive drafting cost. Unless otherwise stated, all ablations use Vicuna-7B evaluated on MT-Bench. We first analyze how to capture the wall-clock advantage of the memory-adaptive design, and then study how the drafting horizon  $\bar{\gamma}$  trades off accepted length against additional loop latency and memory traffic.

### 5.2.1 Memory Budget Analysis

**Adaptivity across memory budgets.** A key advantage of CATS is that the shallow-verifier depth  $L_{SV}$  is a free parameter (Section 5.2.1, properties (i)–(ii)) and can therefore be tuned to fully consume whatever DRAM budget the deployment platform offers, without changing the rest of the pipeline. We exercise this property on three representative edge-memory budgets covering tightly to comfortably resourced devices—2 GB, 6 GB, and 8 GB—and at each budget configure CATS with the deepest  $L_{SV}$  that fits. Table 3 reports per-token compute time, mean accepted length, tokens/s, and end-to-end speedup over the non-speculative baseline. Across all three regimes, CATS achieves the highest speedup, demonstrating that its advantage is not an artifact of one specific memory configuration but a structural benefit that adapts to the available budget.

A natural fix for Kangaroo’s limited acceptance is to deepen its draft model. However, because the draft path is invoked  $\bar{\gamma}$  times per cycle, deepening it amplifies both the repeated DRAM $\leftrightarrow$ on-chip transfer cost and the per-cycle compute load—an overhead that is non-negligible on edge devices.

Table 3: Acceleration under different memory budgets on Vicuna-7B.

Budget	Method	Comp/tok (s)	Mean acc.	Tok/s $\uparrow$	Speedup
2 GB	Baseline	0.213	1.00	0.117	1.00 $\times$
2 GB	Kangaroo ( $L_{DM}=3$ )	0.094	2.27	0.266	2.27 $\times$
2 GB	CATS ( $L_{DM}=3, L_{SV}=5$ )	<b>0.067</b>	<b>2.80</b>	<b>0.329</b>	<b>2.82<math>\times</math></b>
6 GB	Baseline	0.204	1.00	0.126	1.00 $\times$
6 GB	Kangaroo ( $L_{DM}=3$ )	0.089	2.27	0.267	2.12 $\times$
6 GB	CATS ( $L_{DM}=3, L_{SV}=10$ )	<b>0.064</b>	<b>2.94</b>	<b>0.373</b>	<b>2.96<math>\times</math></b>
8 GB	Baseline	0.253	1.00	0.146	1.00 $\times$
8 GB	Kangaroo ( $L_{DM}=3$ )	0.098	2.27	0.282	1.93 $\times$
8 GB	CATS ( $L_{DM}=3, L_{SV}=15$ )	<b>0.062</b>	<b>3.05</b>	<b>0.461</b>	<b>3.16<math>\times</math></b>

We quantify this with *Bytes Per Token* (BPT) [2], the average weight volume streamed from DRAM per generated token. For a two-stage Kangaroo-style pipeline,

$$\text{BPT}_{\text{Kangaroo}} = \frac{\bar{\gamma} \cdot B_{\text{draft}} + B_{\text{verify}}}{\bar{\beta} + 1}, \quad (3)$$

where  $B_{\text{draft}}, B_{\text{verify}}$  are draft and verification parameter volumes and  $\bar{\gamma}$  is drafting passes per cycle. CATS’s three-stage pipeline inserts a shallow verifier, splitting  $B_{\text{verify}}$  into two contiguous segments:

$$\text{BPT}_{\text{CATS}} = \frac{\bar{\gamma} \cdot B_{\text{draft}} + B_{SV} + B_{\text{target}}}{\bar{\beta} + 1}, \quad (4)$$

with  $B_{SV} + B_{\text{target}} = B_{\text{verify}}$ . Because  $B_{SV}$  is streamed once per cycle as part of the target forward pass, enlarging  $L_{SV}$  increases verifier capacity without inflating the  $\bar{\gamma} \cdot B_{\text{draft}}$  term.

Table 4 validates this on Jetson AGX Orin (Vicuna-7B, 8 GB budget). Deepening Kangaroo from  $L_{DM}=3$  to 15 raises  $\bar{\beta}+1$  from 2.27 to 2.98, yet speedup *falls* from 1.93 $\times$  to 1.53 $\times$  as BPT climbs from 8.37 to 11.10 GB/tok. CATS ( $L_{DM}=3, L_{SV}=15$ ) instead achieves similar acceptance (3.05) with the lowest BPT (5.84 GB/tok), and the best speedup (3.16 $\times$ ), confirming that intermediate-layer verification—not a deeper drafter—is the key to edge throughput.

Table 4: Same-budget edge ablation on NVIDIA AGX Orin (Vicuna-7B). Deepening Kangaroo’s draft model improves accepted length but increases BPT and compute cost, while CATS achieves the best speedup with a shallow drafter and single-pass shallow verification.

Method	BPT (GB/tok) $\downarrow$	Comp/tok (s)	Mean acc.	Tok/s $\uparrow$	Speedup
Baseline ( $L=32$ )	12.95	0.253	1.00	0.146	1.00 $\times$
Kangaroo ( $L_{DM}=3$ )	8.37	0.098	2.27	0.282	1.93 $\times$
Kangaroo ( $L_{DM}=5$ )	8.67	0.090	2.41	0.275	1.88 $\times$
Kangaroo ( $L_{DM}=15$ )	11.10	0.106	2.98	0.224	1.53 $\times$
CATS ( $L_{DM}=3, L_{SV}=15$ )	<b>5.84</b>	<b>0.062</b>	<b>3.05</b>	<b>0.461</b>	<b>3.16<math>\times</math></b>

### 5.2.2 Drafting Steps Ablation

We next vary the drafting horizon  $\bar{\gamma}$  to justify the default choice  $\bar{\gamma}=5$ . Increasing  $\bar{\gamma}$  gives the draft stage more opportunities to propose tokens, but it also lengthens the autoregressive drafting loop and increases the streamed volume in the BPT numerator. Table 5 shows this trade-off: moving CATS from  $\bar{\gamma}=3$  to 5 substantially improves accepted length from 2.7077 to 3.0520 with only a small BPT increase, whereas further extending the horizon to 7 or 10 yields diminishing acceptance gains while BPT continues to rise. We therefore use  $\bar{\gamma}=5$  as a balanced setting that captures most of the acceptance benefit before the drafting horizon reaches saturation, while avoiding unnecessary loop latency and memory traffic.

Table 5: Drafting-horizon ablation on Vicuna-7B, reporting accepted length, BPT, and speedup.

$\bar{\gamma}$	Kangaroo			EAGLE-self			CATS		
	Mean acc.	BPT↓	Speedup	Mean acc.	BPT↓	Speedup	Mean acc.	BPT↓	Speedup
3	2.2501	11.1531	1.75×	2.2475	11.1660	1.73×	<b>2.7077</b>	<b>5.6805</b>	<b>2.82×</b>
5	2.4863	13.3496	1.92×	2.5151	13.1967	1.90×	<b>3.0520</b>	<b>5.8354</b>	<b>3.16×</b>
7	2.6330	15.6804	2.04×	2.6194	15.7618	2.00×	<b>3.2343</b>	<b>6.2574</b>	<b>3.34×</b>
10	2.7142	19.6852	2.09×	2.6984	19.8004	2.05×	<b>3.3332</b>	<b>7.1646</b>	<b>3.43×</b>

## 6 Conclusion and Limitations

CATS addresses the flash-transfer bottleneck of memory-limited LLM inference through a staged verification cascade adapted to the device’s DRAM capacity and weight-offloading schedule, raising both token acceptance and end-to-end speedup while keeping the on-device memory footprint equal to that of the target model. Across four target models and five benchmarks, CATS delivers up to 5.08× wall-clock speedup with no quality degradation. Several limitations remain: our evaluation is restricted to 7B–13B models; the draft sub-network and SV adapter rely on distilled adapters, incurring an up-front training cost; and the three-stage design presumes transformer-style layer-aligned representations, restricting direct applicability to architectures such as state-space models.

## References

- [1] Prabhu Vellaisamy, Suresh Tripathi, Vignesh Natarajan, Surya Santhana Thenrasu, Shawn Blanton, and John P. Shen. TaxBreak: Unmasking the hidden costs of LLM inference through overhead decomposition. *arXiv preprint arXiv:2603.12465*, 2026.
- [2] Keivan Alizadeh, Iman Mirzadeh, Dmitry Belenko, S. Karen Khatamifard, Minsik Cho, Carlo C. Del Mundo, Mohammad Rastegari, and Mehrdad Farajtabar. LLM in a flash: Efficient large language model inference with limited memory. In *Proceedings of the 62nd Annual Meeting of the Association for Computational Linguistics (Volume 1: Long Papers)*. Association for Computational Linguistics, 2024.
- [3] Yaniv Leviathan, Matan Kalman, and Yossi Matias. Fast inference from transformers via speculative decoding. In *Proceedings of the 40th International Conference on Machine Learning*, volume 202 of *Proceedings of Machine Learning Research*. PMLR, 2023.
- [4] Charlie Chen, Sebastian Borgeaud, Geoffrey Irving, Jean-Baptiste Lespiau, Laurent Sifre, and John Jumper. Accelerating large language model decoding with speculative sampling. *arXiv preprint arXiv:2302.01318*, 2023.
- [5] Mitchell Stern, Noam Shazeer, and Jakob Uszkoreit. Blockwise parallel decoding for deep autoregressive models. In *Advances in Neural Information Processing Systems*, volume 31, 2018.
- [6] Jun Zhang, Jue Zeng, Huizhen Wang, Linjun Hu, Heming Xia, Tao Ge, and Furu Wei. Draft & verify: Lossless large language model acceleration via self-speculative decoding. In *Proceedings of the 62nd Annual Meeting of the Association for Computational Linguistics (Volume 1: Long Papers)*. Association for Computational Linguistics, 2024.
- [7] Mostafa Elhoushi, Akshat Shrivastava, Diana Liskovich, Basil Hosmer, Bram Wasti, Liangzhen Lai, Anas Mahmoud, Bilge Acun, Saurabh Agarwal, Ahmed Roman, Kelly Ma, and Elias Aly. LayerSkip: Enabling early exit inference and self-speculative decoding. In *Proceedings of the 62nd Annual Meeting of the Association for Computational Linguistics (Volume 1: Long Papers)*. Association for Computational Linguistics, 2024.
- [8] Heming Xia, Yongqi Li, Jun Zhang, Cunxiao Du, and Wenjie Li. SWIFT: On-the-fly self-speculative decoding for LLM inference acceleration. In *The Thirteenth International Conference on Learning Representations*, 2025.
- [9] Fangcheng Liu, Yehui Tang, Zhenhua Liu, Yunsheng Ni, Kai Han, and Yunhe Wang. Kangaroo: Lossless self-speculative decoding via double early exiting. In *Proceedings of the 41st International Conference on Machine Learning*, volume 235 of *Proceedings of Machine Learning Research*. PMLR, 2024.
- [10] Tianle Cai, Yuhong Li, Zhengyang Geng, Hongwu Peng, Jason D. Lee, Deming Chen, and Tri Dao. Medusa: Simple LLM inference acceleration framework with multiple decoding heads. In *Proceedings of the 41st International Conference on Machine Learning*, volume 235 of *Proceedings of Machine Learning Research*. PMLR, 2024.

- [11] Yuhui Li, Fangyun Wei, Chao Zhang, and Hongyang Zhang. EAGLE: Speculative sampling requires rethinking feature uncertainty. In *Proceedings of the 41st International Conference on Machine Learning*, volume 235 of *Proceedings of Machine Learning Research*. PMLR, 2024.
- [12] Heming Xia, Tao Ge, Peiyi Wang, Si-Qing Chen, Furu Wei, and Zhifang Sui. Speculative decoding: Exploiting speculative execution for accelerating Seq2seq generation. In *Findings of the Association for Computational Linguistics: EMNLP 2023*. Association for Computational Linguistics, 2023.
- [13] Xupeng Miao, Gabriele Oliaro, Zhihao Zhang, Xinhao Cheng, Zeyu Wang, Zhengxin Zhang, Rae Ying Yee Wong, Alan Zhu, Lijie Yang, Xiaoxiang Shi, Chunan Shi, Zhuoming Chen, Daiyaan Arfeen, Reyna Abhyankar, and Zhihao Jia. SpecInfer: Accelerating large language model serving with tree-based speculative inference and verification. In *Proceedings of the 29th ACM International Conference on Architectural Support for Programming Languages and Operating Systems, Volume 3*, ASPLOS '24. ACM, 2024.
- [14] Zhuoming Chen, Avner May, Ruslan Svirschevski, Yuhsun Huang, Max Ryabinin, Zhihao Jia, and Beidi Chen. Sequoia: Scalable, robust, and hardware-aware speculative decoding. In *Advances in Neural Information Processing Systems*, volume 37, 2024.
- [15] Jikai Wang, Yi Su, Juntao Li, Qingrong Xia, Zi Ye, Xinyu Duan, Zhefeng Wang, and Min Zhang. OPT-Tree: Speculative decoding with adaptive draft tree structure. *arXiv preprint arXiv:2406.17276*, 2024.
- [16] Yunfan Xiong, Ruoyu Zhang, Yanzeng Li, Tianhao Wu, and Lei Zou. DySpec: Faster speculative decoding with dynamic token tree structure. *arXiv preprint arXiv:2410.11744*, 2024.
- [17] Yongchao Zhou, Kaifeng Lyu, Ankit Singh Rawat, Aditya Krishna Menon, Afshin Rostamizadeh, Sanjiv Kumar, Jean-François Kagy, and Rishabh Agarwal. DistillSpec: Improving speculative decoding via knowledge distillation. In *The Twelfth International Conference on Learning Representations*, 2024.
- [18] Xiaoxuan Liu, Lanxiang Qian, Ying Ye, Qinghao Zhao, Joseph E. Gonzalez, Ion Stoica, and Hao Zhang. Online speculative decoding. In *Proceedings of the 41st International Conference on Machine Learning*, volume 235 of *Proceedings of Machine Learning Research*. PMLR, 2024.
- [19] Cunxiao Du, Jing Jiang, Yuankai Xu, Jiawei Wu, Sicheng Yu, Yongqi Li, Shenggui Li, Kai Xu, Liqiang Nie, Zhaopeng Tu, and Yang You. GliDe with a CaPE: A low-hassle method to accelerate speculative decoding. In *Proceedings of the 41st International Conference on Machine Learning*, volume 235 of *Proceedings of Machine Learning Research*. PMLR, 2024.
- [20] Zhenyu He, Zexuan Zhong, Tianle Cai, Jason D. Lee, and Di He. REST: Retrieval-based speculative decoding. In *Proceedings of the 2024 Conference of the North American Chapter of the Association for Computational Linguistics: Human Language Technologies*, NAACL 2024. Association for Computational Linguistics, 2024.
- [21] Minghan Li, Xilun Chen, Ari Holtzman, Beidi Chen, Jimmy Lin, Wen-tau Yih, and Xi Victoria Lin. Nearest neighbor speculative decoding for LLM generation and attribution. In *Advances in Neural Information Processing Systems*, volume 37, 2024.
- [22] Gabriele Oliaro, Zhihao Jia, Daniel Campos, and Aurick Qiao. SuffixDecoding: A model-free approach to speeding up large language model inference. In *Advances in Neural Information Processing Systems*, volume 38, 2025.
- [23] Yichao Fu, Peter Bailis, Ion Stoica, and Hao Zhang. Break the sequential dependency of LLM inference using lookahead decoding. *arXiv preprint arXiv:2402.02057*, 2024.
- [24] Heming Xia, Zhe Yang, Qingxiu Dong, Peiyi Wang, Yongqi Li, Tao Ge, Tianyu Liu, Wenjie Li, and Zhifang Sui. Unlocking efficiency in large language model inference: A comprehensive survey of speculative decoding. In *Findings of the Association for Computational Linguistics: ACL 2024*. Association for Computational Linguistics, 2024.
- [25] Sehoon Kim, Karttikeya Mangalam, Suhong Moon, Jitendra Malik, Michael W. Mahoney, Amir Gholami, and Kurt Keutzer. Speculative decoding with big little decoder. In *Advances in Neural Information Processing Systems*, volume 36, 2023.
- [26] Ziyi Chen, Xiaocong Yang, Jiacheng Lin, Chenkai Sun, Kevin Chen-Chuan Chang, and Jie He. Cascade speculative drafting for even faster LLM inference. In *Advances in Neural Information Processing Systems*, volume 37, 2024.

- [27] Weilin Zhao, Yuxiang Huang, Xu Han, Wang Xu, Chaojun Xiao, Zhiyuan Liu, and Maosong Sun. Ouroboros: Speculative decoding with large model enhanced drafting. In *Proceedings of the 2024 Conference on Empirical Methods in Natural Language Processing*. Association for Computational Linguistics, 2024.
- [28] Zilong Wang, Zifeng Wang, Long Le, Huaixiu Steven Zheng, Swaroop Mishra, Vincent Perot, Yuwei Zhang, Anush Goldie, Jingbo Shang, Chenguang Zhu, Chen-Yu Lee, and Tomas Pfister. Speculative RAG: Enhancing retrieval augmented generation through drafting. In *The Thirteenth International Conference on Learning Representations*, 2025.
- [29] Meiyu Zhong, Noel Teku, and Ravi Tandon. Speeding up speculative decoding via sequential approximate verification. In *Proceedings of the 3rd Efficient Systems for Foundation Models Workshop at the 42nd International Conference on Machine Learning*, volume 267 of *Proceedings of Machine Learning Research*. PMLR, 2025.
- [30] Ziteng Sun, Ananda Theertha Suresh, Jae Hun Ro, Ahmad Beirami, Himanshu Jain, and Felix Yu. SpecTr: Fast speculative decoding via optimal transport. In *Advances in Neural Information Processing Systems*, volume 36, 2023.
- [31] Ziteng Sun, Jae Hun Ro, Ahmad Beirami, and Ananda Theertha Suresh. Block verification accelerates speculative decoding. In *The Thirteenth International Conference on Learning Representations*, 2025.
- [32] Gregor Bachmann, Sotiris Anagnostidis, Albert Pumarola, Markos Georgopoulos, Artsiom Sanakoyeu, Yuming Du, Edgar Schönfeld, Ali Thabet, and Jonas Kohler. Judge decoding: Faster speculative sampling requires going beyond model alignment. In *The Thirteenth International Conference on Learning Representations*, 2025.
- [33] Yixuan Wang, Yijun Liu, Shiyu Ji, Yuzhuang Xu, Yang Xu, Qingfu Zhu, and Wanxiang Che. Think before you accept: Semantic reflective verification for faster speculative decoding. *arXiv preprint arXiv:2505.18629*, 2025.
- [34] Hanshi Sun, Zhuoming Chen, Xinyu Yang, Yuandong Tian, and Beidi Chen. TriForce: Lossless acceleration of long sequence generation with hierarchical speculative decoding. In *First Conference on Language Modeling*, 2024.
- [35] Jian Chen, Vashisth Tiwari, Ranajoy Sadhukhan, Zhuoming Chen, Jinyuan Shi, Ian En-Hsu Yen, and Beidi Chen. MagicDec: Breaking the latency-throughput tradeoff for long context generation with speculative decoding. In *The Thirteenth International Conference on Learning Representations*, 2025.
- [36] Seongjin Cha, Gyuwan Kim, Dongsu Han, Tao Yang, and Insu Han. KnapSpec: Self-speculative decoding via adaptive layer selection as a knapsack problem. *arXiv preprint arXiv:2602.20217*, 2026.
- [37] Zachary Ankner, Rishab Parthasarathy, Aniruddha Nrusimha, Christopher Rinard, Jonathan Ragan-Kelley, and William Brandon. Hydra: Sequentially-dependent draft heads for Medusa decoding. In *First Conference on Language Modeling*, 2024.
- [38] Yuhui Li, Fangyun Wei, Chao Zhang, and Hongyang Zhang. EAGLE-2: Faster inference of language models with dynamic draft trees. In *The Thirteenth International Conference on Learning Representations*, 2025.
- [39] Yuhui Li, Fangyun Wei, Chao Zhang, and Hongyang Zhang. EAGLE-3: Scaling up inference acceleration of large language models via training-time test. In *Advances in Neural Information Processing Systems*, volume 38, 2025.
- [40] Siqi Kou, Lanxiang Hu, Zhezhi He, Zhijie Deng, and Hao Zhang. CLLMs: Consistency large language models. In *Proceedings of the 41st International Conference on Machine Learning*, volume 235 of *Proceedings of Machine Learning Research*. PMLR, 2024.
- [41] Gabe Guo and Stefano Ermon. Self-speculative decoding in any-order and any-subset autoregressive models. In *Structured Probabilistic Inference and Generative Modeling Workshop at NeurIPS 2025*, 2025.
- [42] Fabian Gloeckle, Badr Youbi Idrissi, Baptiste Rozière, David Lopez-Paz, and Gabriel Synnaeve. Better & faster large language models via multi-token prediction. In *Proceedings of the 41st International Conference on Machine Learning*, volume 235 of *Proceedings of Machine Learning Research*. PMLR, 2024.
- [43] Zongyue Qin, Ziniu Hu, Zifan He, Neha Prakriya, Jason Cong, and Yizhou Sun. Multi-token joint speculative decoding for accelerating large language model inference. *arXiv preprint arXiv:2407.09722*, 2024.

- [44] Giovanni Monea, Armand Joulin, and Edouard Grave. PaSS: Parallel speculative sampling. In *Efficient Natural Language and Speech Processing Workshop at NeurIPS 2023*, 2023.
- [45] Yixin Song, Zeyu Mi, Haotong Xie, and Haibo Chen. PowerInfer: Fast large language model serving with a consumer-grade GPU. In *Proceedings of the ACM SIGOPS 30th Symposium on Operating Systems Principles*. ACM, 2024.
- [46] Zebin Ren, Krijn Doekemeijer, Tiziano De Matteis, Christian Pinto, Radu Stoica, and Animesh Trivedi. An I/O characterizing study of offloading LLM models and KV caches to NVMe SSD. In *Proceedings of the Twentieth European Conference on Computer Systems*, EuroSys '25. ACM, 2025.
- [47] Hao Chen, Cong Tian, Zixuan He, Bin Yu, Yepang Liu, and Jialun Cao. Inference performance evaluation for LLMs on edge devices with a novel benchmarking framework and metric. *arXiv preprint arXiv:2508.11269*, 2025.
- [48] Wei-Lin Chiang, Zhuohan Li, Zi Lin, Ying Sheng, Zhanghao Wu, Hao Zhang, Lianmin Zheng, Siyuan Zhuang, Yonghao Zhuang, Joseph E. Gonzalez, Ion Stoica, and Eric P. Xing. Vicuna: An open-source chatbot impressing GPT-4 with 90% ChatGPT quality. <https://lmsys.org/blog/2023-03-30-vicuna/>, 2023.
- [49] Hugo Touvron, Louis Martin, Kevin Stone, Peter Albert, Amjad Almahairi, Yasmine Babaei, Nikolay Bashlykov, Soumya Batra, Prajjwal Bhargava, Shruti Bhosale, et al. Llama 2: Open foundation and fine-tuned chat models. *arXiv preprint arXiv:2307.09288*, 2023.
- [50] Lianmin Zheng, Wei-Lin Chiang, Ying Sheng, Siyuan Zhuang, Zhanghao Wu, Yonghao Zhuang, Zi Lin, Zhuohan Li, Dacheng Li, Eric P. Xing, Hao Zhang, Joseph E. Gonzalez, and Ion Stoica. Judging LLM-as-a-judge with MT-Bench and chatbot arena. In *Advances in Neural Information Processing Systems*, volume 36, 2023.
- [51] Karl Cobbe, Vineet Kosaraju, Mohammad Bavarian, Mark Chen, Heewoo Jun, Lukasz Kaiser, Matthias Plappert, Jerry Tworek, Jacob Hilton, Reiichiro Nakano, Christopher Hesse, and John Schulman. Training verifiers to solve math word problems. *arXiv preprint arXiv:2110.14168*, 2021.
- [52] Rohan Taori, Ishaan Gulrajani, Tianyi Zhang, Yann Dubois, Xuechen Li, Carlos Guestrin, Percy Liang, and Tatsunori B. Hashimoto. Stanford Alpaca: An instruction-following LLaMA model. [https://github.com/tatsu-lab/stanford\\_alpaca](https://github.com/tatsu-lab/stanford_alpaca), 2023.
- [53] Mark Chen, Jerry Tworek, Heewoo Jun, Qiming Yuan, Henrique Ponde de Oliveira Pinto, Jared Kaplan, Harri Edwards, Yuri Burda, Nicholas Joseph, Greg Brockman, et al. Evaluating large language models trained on code. *arXiv preprint arXiv:2107.03374*, 2021.

## A CATS algorithm

---

### Algorithm 1 CATS: Cascaded Self-Speculative Decoding with Tree-Masked Final Verification

---

**Require:** Prompt  $\mathbf{x}$ ; target model  $\mathcal{M}$  with layers  $1:L_{\text{total}}$  and LM head  $\mathcal{H}$ ; draft cut-point  $L_{\text{DM}}$ , shallow-verifier cut-point  $L_{\text{SV}}$  ( $1 \leq L_{\text{DM}} < L_{\text{SV}} < L_{\text{total}}$ ); draft adapter  $\mathcal{A}_{\text{DM}}$ , SV adapter  $\mathcal{A}_{\text{SV}}$ ; drafting horizon  $\bar{\gamma}$ ; max new tokens  $T$ ; acceptance criterion ACC (greedy or typical [10])

**Ensure:** Generated sequence  $\mathbf{y}$

```

1: // ===== Initialization =====
2: Load layers  $1:L_{\text{SV}}$  (DM  $\cup$  SV) into DRAM and pin resident
3:  $(\mathbf{h}^{(1:L_{\text{total}})}, \text{KV}_{\mathcal{M}}) \leftarrow \mathcal{M}(\mathbf{x})$  ▷ prompt prefill, full target
4:  $y_0 \leftarrow \arg \max \mathcal{H}(\mathbf{h}_{-1}^{(L_{\text{total}})})$ ; initialize  $\text{KV}_{\mathcal{A}_{\text{DM}}}, \text{KV}_{\mathcal{A}_{\text{SV}}}$  from  $\mathbf{h}^{(L_{\text{DM}})}, \mathbf{h}^{(L_{\text{SV}})}$ 
5:  $s \leftarrow |\mathbf{x}|$  ▷ committed length

6: while  $s < T$  do
7:   // ===== Stage 1: Draft =====
8:    $\mathbf{d} \leftarrow []$ ;  $\mathbf{H}_{\text{DM}} \leftarrow []$ 
9:   for  $k = 0, \dots, \bar{\gamma}-1$  do
10:     $h \leftarrow \mathcal{M}_{1:L_{\text{DM}}}(y_{s+k}, \text{KV}_{\mathcal{M}})$ ; append  $h$  to  $\mathbf{H}_{\text{DM}}$ 
11:     $(o, \text{KV}_{\mathcal{A}_{\text{DM}}}) \leftarrow \mathcal{A}_{\text{DM}}(h, \text{KV}_{\mathcal{A}_{\text{DM}}})$ 
12:     $y_{s+k+1} \leftarrow \arg \max \mathcal{H}(o)$ ; append to  $\mathbf{d}$ 
13:   end for

14:   // ===== Stage 2: Shallow Verification =====
15:    $\mathbf{H}_{\text{SV}} \leftarrow \mathcal{M}_{L_{\text{DM}}+1:L_{\text{SV}}}(\mathbf{H}_{\text{DM}}, \text{KV}_{\mathcal{M}})$  ▷  $\bar{\gamma}$  positions in parallel
16:    $(\mathbf{O}_{\text{SV}}, \text{KV}_{\mathcal{A}_{\text{SV}}}) \leftarrow \mathcal{A}_{\text{SV}}(\mathbf{H}_{\text{SV}}, \text{KV}_{\mathcal{A}_{\text{SV}}})$ ;  $\hat{\mathbf{c}} \leftarrow \arg \max \mathcal{H}(\mathbf{O}_{\text{SV}})$ 
17:    $\mathcal{R} \leftarrow \{(i, \hat{c}_i) : \hat{c}_i \neq d_i, 0 \leq i < \bar{\gamma}\}$  ▷ positions where SV proposes a correction

18:   if  $\mathcal{R} = \emptyset$  then
19:      $\mathcal{T} \leftarrow \text{CHAINTREE}(\mathbf{d})$  ▷ straight chain, no correction branches
20:   else
21:      $\mathcal{T} \leftarrow \text{BUILDTREE}(\text{main} = \mathbf{d}, \text{corrections} = \mathcal{R})$ 
22:     ▷ main branch is unchanged; each  $(i, \hat{c}_i) \in \mathcal{R}$  adds a side branch at position  $i$ 
23:     Re-forward correction tokens through layers  $1:L_{\text{SV}}$  under tree-masked attention
24:     ▷ reuses DRAM-resident DM and SV layers; zero additional flash transfer
25:   end if

26:   // ===== Stage 3: Final Verification (stream layers  $L_{\text{SV}}+1:L_{\text{total}}$  from flash) =====
27:    $\mathbf{H}_{\text{tgt}} \leftarrow \mathcal{M}_{L_{\text{SV}}+1:L_{\text{total}}}(\mathcal{T}.\text{hidden\_states}, \text{mask}=\mathcal{T}.\text{tree\_mask}, \text{KV}_{\mathcal{M}})$ 
28:    $\mathbf{p}_{\text{tgt}} \leftarrow \text{softmax}(\mathcal{H}(\mathbf{H}_{\text{tgt}}))$ 

29:   // — Walk the tree to find the longest accepted prefix —
30:    $a \leftarrow 0$ ;  $\mathbf{y}_{\text{out}} \leftarrow []$ 
31:   for  $i = 0, \dots, \bar{\gamma}-1$  do
32:     if  $\text{ACC}(d_i, \mathbf{p}_{\text{tgt}}^{(i)})$  then
33:        $a \leftarrow a + 1$ ; append  $d_i$  to  $\mathbf{y}_{\text{out}}$ 
34:     else if  $(i, \hat{c}_i) \in \mathcal{R}$  and  $\text{ACC}(\hat{c}_i, \mathbf{p}_{\text{tgt}}^{(\text{corr}, i)})$  then
35:        $a \leftarrow a + 1$ ; append  $\hat{c}_i$  to  $\mathbf{y}_{\text{out}}$ ; break ▷ correction branch terminates the cycle by construction
36:     else
37:       break
38:     end if
39:   end for
40:   Append  $\arg \max \mathbf{p}_{\text{tgt}}^{(a)}$  to  $\mathbf{y}_{\text{out}}$  ▷ bonus token from target's own next-token prediction

41:   Commit  $\mathbf{y}_{\text{out}}$  to  $\mathbf{y}$ ;  $s \leftarrow s + |\mathbf{y}_{\text{out}}|$ 
42:   Roll back  $\text{KV}_{\mathcal{M}}, \text{KV}_{\mathcal{A}_{\text{DM}}}, \text{KV}_{\mathcal{A}_{\text{SV}}}$  to length  $s$  along the accepted path
43: end while
44: return  $\mathbf{y}_{0:s}$ 

```

---

## B Reduced KL Loss Computation Process

In this appendix we expand the construction of the **Reduced KL Loss** introduced in Section 4, Equation 2. Recall the setup: we train the draft and shallow-verifier adapters by aligning their output distribution  $q_{\text{draft}}(v | t)$  with the target-model distribution  $p_{\text{target}}(v | t)$  across a set  $M$  of unmasked token positions, where  $v \in \{1, \dots, V\}$  indexes vocabulary tokens and  $t$  indexes positions. The standard full-vocabulary distillation loss in Equation 1,

$$\mathcal{L}_{\text{full}} = -\frac{1}{|M|} \sum_{t \in M} \sum_{v=1}^V p_{\text{target}}(v | t) \cdot \log q_{\text{draft}}(v | t),$$

spreads supervision over all  $V$  tokens, but the vast majority of vocabulary mass at any position  $t$  sits in a long tail of near-zero probabilities that rarely determines acceptance. To concentrate the limited capacity of our compact adapters on the tokens that actually matter, we restrict the loss to the top- $K$  tokens of  $p_{\text{target}}(\cdot | t)$  at each position. The construction proceeds in three steps.

**Step 1: Select the top- $K$  indices.** At each unmasked position  $t \in M$ , identify the  $K$  vocabulary tokens carrying the highest probability mass under the target distribution:

$$\mathcal{T}_K(t) = \arg \text{top-}K_{v \in \{1, \dots, V\}} p_{\text{target}}(v | t). \quad (5)$$

$\mathcal{T}_K(t)$  is a position-dependent support of size  $|\mathcal{T}_K(t)| = K$  that captures the tokens with non-negligible probability of being emitted by the target model. In speculative decoding, only tokens within this set can plausibly be accepted, so any supervision spent outside  $\mathcal{T}_K(t)$  is effectively wasted.

**Step 2: Renormalize over the focused support.** The masses  $\{p_{\text{target}}(v | t)\}_{v \in \mathcal{T}_K(t)}$  in general do not sum to 1. We renormalize them onto  $\mathcal{T}_K(t)$  to obtain a valid probability distribution  $\tilde{p}_{\text{target}}(v | t)$ :

$$\tilde{p}_{\text{target}}(v | t) = \begin{cases} \frac{p_{\text{target}}(v | t)}{\sum_{v' \in \mathcal{T}_K(t)} p_{\text{target}}(v' | t)}, & v \in \mathcal{T}_K(t), \\ 0, & v \notin \mathcal{T}_K(t). \end{cases} \quad (6)$$

Equivalently, with an indicator function  $\mathbf{1}[\cdot]$ :

$$\tilde{p}_{\text{target}}(v | t) = \frac{p_{\text{target}}(v | t) \cdot \mathbf{1}[v \in \mathcal{T}_K(t)]}{\sum_{v' \in \mathcal{T}_K(t)} p_{\text{target}}(v' | t)}. \quad (7)$$

By construction  $\sum_{v=1}^V \tilde{p}_{\text{target}}(v | t) = 1$ , so  $\tilde{p}_{\text{target}}(\cdot | t)$  is a proper distribution supported on  $\mathcal{T}_K(t)$  and zero elsewhere.

**Step 3: Cross-entropy on the focused support.** The Reduced KL Loss is the position-averaged cross-entropy between  $\tilde{p}_{\text{target}}(\cdot | t)$  and the adapter distribution  $q_{\text{draft}}(\cdot | t)$ , evaluated only on  $\mathcal{T}_K(t)$ :

$$\mathcal{L}_{\text{top-}K} = -\frac{1}{|M|} \sum_{t \in M} \sum_{v \in \mathcal{T}_K(t)} \tilde{p}_{\text{target}}(v | t) \cdot \log q_{\text{draft}}(v | t). \quad (8)$$

Because  $\tilde{p}_{\text{target}}(v | t) = 0$  for  $v \notin \mathcal{T}_K(t)$ , the inner sum is mathematically equivalent to summing over the entire vocabulary; in practice we materialize only the  $K$  active terms per position to avoid the  $V-K$  vanishing contributions. Up to a constant entropy term  $H(\tilde{p}_{\text{target}}(\cdot | t))$  that does not depend on the adapter parameters,  $\mathcal{L}_{\text{top-}K}$  coincides with the position-averaged KL divergence

$$\frac{1}{|M|} \sum_{t \in M} \text{KL}(\tilde{p}_{\text{target}}(\cdot | t) \parallel q_{\text{draft}}(\cdot | t)),$$

which is why we call it the *Reduced* KL Loss: it is a KL divergence taken over a reduced support  $\mathcal{T}_K(t)$  rather than the full vocabulary  $V$ .

**Effect on adapter training.** Compared with  $\mathcal{L}_{\text{full}}$ , restricting supervision to  $\mathcal{T}_K(t)$  has two effects. First, it concentrates gradient signal on the candidates that drive acceptance, since tokens outside  $\mathcal{T}_K(t)$  have  $p_{\text{target}}$  values too small to be accepted regardless of how  $q_{\text{draft}}$  allocates mass to them. Second, it stabilizes training under our compact draft and shallow-verifier sub-networks: the long tail of near-zero target probabilities no longer consumes adapter capacity. This is essential in our memory-limited setting, where the draft and SV sub-networks must remain small enough to fit in the DRAM budget while still producing high-acceptance candidates.